Burning Paper: Simulation at the Fiber's Level

Caroline Larboulette,* Pablo Quesada† and Olivier Dumas‡
University of South Brittany & University of Santiago de Compostela

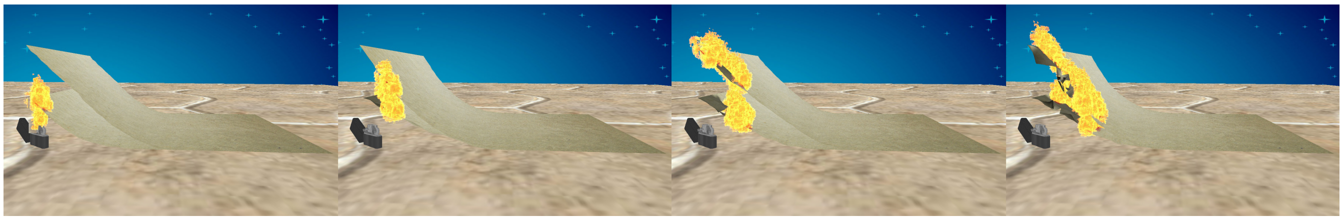

Figure 1: *Simulation of a burning stack of paper sheets. From left to right: the bottom sheet is put on fire; the fire propagates to the top sheet; the burning process continues.*

Abstract

This paper presents a novel physically based algorithm that simulates the deformation of paper when it burns. We use a particle system to represent the fire and a mass-spring system coupled to a heat propagation solver to deform the polygonal mesh representing the paper sheet. When burnout, the paper becomes non-elastic and fractures automatically occur where the stress is important. By tuning the physical parameters of size, grammage, density, dimensional stability, specific heat and thermal conductivity, we are able to simulate the crumpling and burning of various types of paper as we show with our results.

CR Categories: I.3.7 [Computer Graphics]: Three-Dimensional Graphics and Realism—Animation;

Keywords: paper, burning, crumpling, heat diffusion, particle system, mass-spring system, fracture

1 Introduction

Some natural phenomena such as the burning of objects are too dangerous or too costly to be filmed for a movie or used in a video game. It is thus important to develop Computer Graphics algorithms capable of simulating those effects.

Instead of simulating the crumpling and burning behavior of the paper using manually controlled tools such as Free Form Deformations (FFD) [Melek and Keyser 2006], we propose an algorithm to simulate this behavior from the paper fibers' properties inside a physically based simulation.

We propose a mapping of paper's properties of size, grammage, stability, heat capability and thermal conductivity to the simulation parameters. The main advantage of our approach over previous work is that different kinds of paper with different shapes can be represented by only changing the simulation parameters, that is, the paper properties.

We use a heat diffusion process and a particle system to guide a mass-spring simulation. The propagating heat is responsible for changes in the rest length of the fibers represented by the springs. The mass-spring simulation results in crumpling and bending effects. Figure 7 shows a comparison between real paper burning and our simulation.

Section 2 reviews related work. Section 3 describes the properties of the paper that are involved in the burning process and section 4 details our framework and the mapping of the properties to the simulation parameters. Section 5 shows some results and section 6 concludes and discusses future work.

2 Related Work

Very little previous work exist regarding the burning of objects, and, more specifically concerning paper crumpling and burning.

[Carlson et al. 2002] and [Matsumura and Tsuruno 2006] treat solids as fluids with a variable viscosity for melting effects. The deformation is computed using fluid dynamics and solving the Navier-Stokes equations, but the wear of the materials is not taken into account. To this end, Losasso et al. [Losasso et al. 2006] use a triangle mesh for paper representation and re-mesh the boundary to smooth the deformation due to the action of fire. The wear of the material is transformed into fire combustible like in [Nguyen et al. 2002].These techniques are costly and are not capable of representing secondary effects like bending or crumpling due to internal forces.

Regarding the combustion and decomposition of objects, fire and heat propagation are directly related to the burning process. Melek et al. [Melek and Keyser 2003; Melek and Keyser 2004; Melek and Keyser 2006; Melek and Keyser 2007] present a simple model for decomposition and deformation of objects, using a heat equation for modeling the diffusion process. In [Melek and Keyser 2006] they propose a FFD-based method for modeling minor structural changes of small burning objects. They place a lattice around the object and compute a weighted deformation based on the contraction of the lattice associated to a cosine function to generate crumpling effects. We also use a heat equation to model the diffusion process, but it is coupled to a mass-spring system to compute the deformation.

Liu et al. [Liu et al. 2009] simulate a gradient-based fire spreading to compute the distribution of temperature. They also use a FFD

*e-mail:caroline.larboulette@gmail.com
†e-mail:pabloqb@gmail.com
‡e-mail:olivier.dumas@gmx.fr

Motion in Games 2013, November 7 – 9, 2013, Dublin, Ireland.

ACM 978-1-4503-2546-2/13/11 $15.00

technique to crumple and bend the paper by rotating the control vertices of a mass-spring lattice.

Both techniques generate visually plausible results of bending and crumpling deformations but the deformations are procedurally defined and do not take into account the physics of the burning process. Different lattices and deformation techniques need to be defined for different types of materials like matches or paper even when both objects have a similar internal structure based on fibers.

Jeong et al. [Jeong et al. 2011] use a two-layer beam model with springs and also change the springs length during the simulation, but this change is induced by a loss of mass. In our simulation, although the nodes also lose mass when burning, the change of springs rest length depends on the temperature of the nodes and is what drives the crumpling deformation. Another major difference is that we do not lose the paper material entirely when it burns, it shrinks and fractures but the material is still there as ashes. In addition, we do model the fire, so we are able to, for example, burn a stack of paper, something previous techniques that do not simulate the fire cannot achieve.

On the other hand, extensive research exists on mass-spring simulation of thin objects, such as cloth simulation. An overview of existing techniques can be found in [Nealen et al. 2005]. In our approach, we use a standard cloth simulation lattice [Provot 1995] with an explicit Runge-Kutta of order four integration technique. We use the springs of the lattice to represent the fibers of the paper. We obtain different kinds of paper by setting different stiffness values for the springs and different parameters for the heat propagation (section 4). For example, rough paper like cardboard is simulated with higher stiffness values for the springs.

3 Paper Properties

Dimensions and Grammage At first glance, paper has two main properties: size, i.e. the dimensions of a sheet of paper; and grammage, i.e. the weight in grams of one square meter of paper. Standard ISO $A4$ paper has a size of 21x29.7 cm and a grammage depending on its quality. Printing paper weighs between $60g.m^{-2}$ and $120g.m^{-2}$.

The dimensions and grammage of the paper are directly mapped as parameters of the mass-spring simulation: the grammage defines the mass of the nodes, and the dimensions specify the distance between them.

Fibers Properties Other important properties are the manufacture direction, dimension stability, fibers distribution and fibers quality.

During the manufacture process, from softwood to paper, fibers properties are modified. Length, flexibility and bending ability of fibers turn into stiffness, smoothness and surface strength of the paper.

The way fibers are distributed inside the paper is random due to the pulp of wood used, the manufacture process and the environment conditions, but they are mainly oriented in the manufacture direction (*main direction*) affecting paper properties and have influence on the dimensional stability (see figure 2). Because of this orientation, it is harder to bend the paper across the main direction [Johansson et al. 2011].

The dimensional stability is the ability of a material to keep its original structure when the temperature or the humidity changes. When burning, fibers lose elasticity and change length, which makes the paper crumple. It can also produce a fracture around the boundary of burnt area. Due to its cellulose nature, it is impossible to keep the paper absolutely stable but a good manufacture work can minimize some changes. A paper with higher dimensional stability will be more resistant to bending and crumpling, that is, of better quality.

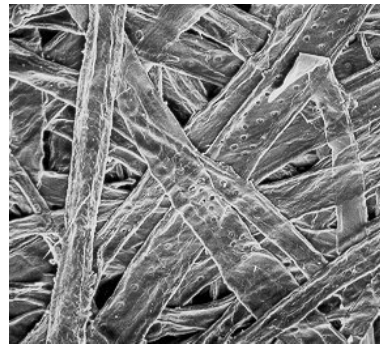

Figure 2: *Fibers composing real paper.*

Other Properties The density, specific heat capability and thermal conductivity are all related to *how fast* a piece of paper burns and are mapped into the heat equation.

4 Our Framework

Our framework relies on the coupling of a mass-spring system to simulate the crumpling behavior of burning paper, a particle system to simulate the fire both from the lighter and generated by the paper when it burns, a heat diffusion process to propagate the heat responsible of the burning, as well as an algorithm to cut the mass-spring system and rendered polygonal mesh to simulate the fracture of burnt paper.

During the simulation, we first add energy to the system by adding heat and forces due to the fire particles. We then update the mass-spring system and solve the heat equation (3). The nodes are updated with the new temperature slowly changing their state from *not burning* to *burning* to *burnout* as a function of heat and time.

Once the heat has been solved on the mesh, we modify the springs length as a function of temperature. Because a fiber loses humidity when burning, it tends to shorten which influences the crumpling effect. We thus reduce the length of the springs according to equation (4) if they connect *burning* nodes at each timestep.

For the rendering of the sheet of paper, we draw quads directly mapped on the mass-spring system: vertices are nodes, and edges are structural springs. Note that the number of quads is constant during simulation.

4.1 Simulation Parameters

We get the parameters for our simulation from paper properties. Some of them have a direct mapping, others need to be combined to be introduced into the simulation.

Grammage and Dimension Our mass-spring system is composed of nodes aligned in horizontal and vertical directions connected by structural, diagonal and bending springs [Provot 1995]. Figure 4 (left) shows the mass-spring system. We use the grammage and dimensions of the sheet of paper to compute the mass of the nodes as well as their relative positions.

Manufacture Direction Using a right-handed coordinates system, the main direction is set to be the x-axis, meanwhile the cross direction is the z-axis. For a MxN grid resolution the nodes are distributed at a distance d_1 and d_2 according to:

$$\begin{array}{ll} M * d_1 = z\,m & \textit{cross direction} \\ N * d_2 = x\,m & \textit{main direction} \end{array} \tag{1}$$

with z being the width of the sheet and x its height in meters.

Fibers as Springs Manufacture direction and dimensional stability do not have a direct mapping into the system. We thus group the structural, diagonal and bending springs by their functionality:

1. *Main Springs*: they represent the fibers.

   Manufacture or Structural Springs: Main and Cross direction of the fibers.

   Adherence or Diagonal Springs: Stability and fibers bonds.

2. *Secondary or Bending Springs*: they are for additional fibers properties.

The rest length of each spring depends on the distance between the nodes it is connected to. Structural springs have a rest length of d_1 and d_2 respectively (see equation (1)). Diagonal springs have a rest length h such that $h^2 = (d_1)^2 + (d_2)^2$. Bending springs have a rest length of $2 * d_1$ and $2 * d_2$ for horizontal and vertical directions respectively.

To obtain the anisotropic crumpling behavior that is due to the fact that fibers in the main direction are longer than fibers in the cross direction, we vary the stiffnesses of the structural springs from a fiber to the next. This variation is applied to both main and cross directions but in a different way. Using the same stiffness per row but different values from one row to the next, we represent the main direction of the paper as we simulate longer fibers (horizontal). Cross direction springs (vertical) use different stiffnesses from one row to the next but the same on a given row simulating shorter fibers (see figure 3).

From an initial value of stiffness depending on the node weight (see below), we tested that a random stiffness of $\pm 10\%$ on the structural springs stiffness keeps the system stable using the same mass and integration timestep and offers a more accurate behavior compared to having no randomness.

$k_{structural} = k_{diagonal} = nodeweight * 7e^3 N.m^{-1}$

$k_{bending} = nodeweight * 2e^4 N.m^{-1}$

Finally, the damping coefficient is the same for all the springs. In our examples, we used a value of $d = nodeweight * 5$.

Dimensional Stability It is a constant c_s representing the quality of the paper. It is introduced in both the heat propagation equation (section 4.2) and fibers deformation (section 4.3). As dimensional stability is a reference of paper quality we map it from $1.e^{-4}$ to $1.e^{-2}$ as a factor to get different paper qualities.

4.2 Burning the Paper

Fire Simulation We model the fire as a standard particle system [Reeves 1983; van der Burg 2000]. Emitters are created to emit the particles with a given velocity and a temperature of 512 ^oC. Over time, the position and the temperature of the particles are updated. We use billboards for rendering: the size is given by the fire particle temperature and the color is given by a texture with an alpha channel. Refer to the teaser for an example.

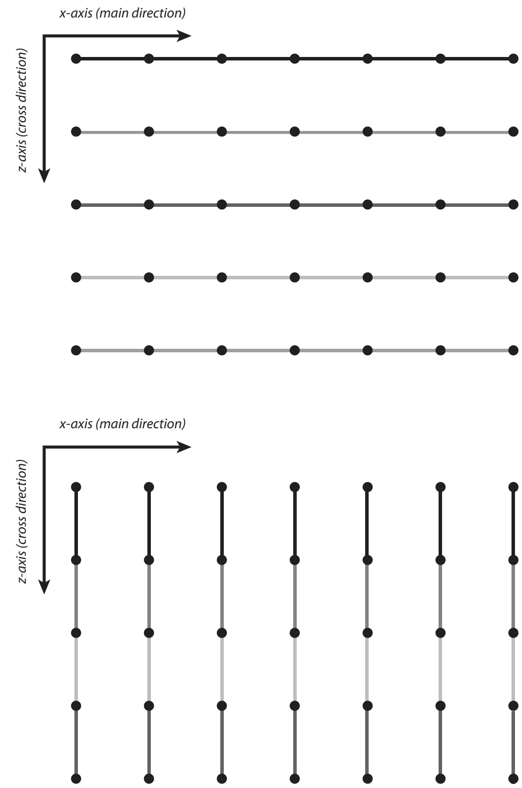

Figure 3: *Stiffness coefficients of the springs (different grays represent different values of stiffness). Top: main direction of the fibers with same stiffness per row; bottom: cross direction with different stiffnesses along a given column.*

Fire particles interact with the mass-spring system. If a particle is close enough to a node of the mass-spring system, it transfers its energy to that node as heat, that is then used for the heat propagation, and an external force f_{ext} is added to the external forces of the mass-spring simulation.

Heat Propagation The heat is propagated using a partial differential equation. The $2D$ equation can be written as:

$$c_s \rho c \frac{\partial u}{\partial t} = D(\frac{\partial^2 u}{\partial x^2} + \frac{\partial^2 u}{\partial y^2}) + s \tag{2}$$

where u is the temperature, c_s the dimensional stability, ρ is the paper density, c is the specific heat capability, D is the thermal conductivity and s an external source term. Table 1 shows the values of the parameters directly related to heat for a standard paper. The density of paper has a value ranging from $0.25 g.m^{-3}$ (*silk paper*) to $1.5 g.m^{-3}$ (*photo quality paper*).

Specific Heat	Thermal Conductivity
$1.38 kJ.kg^{-1}.^oC^{-1}$	$0.05 J.s^{-1}.^oC^{-1}.m^{-1}$

Table 1: *Paper parameters mapped to the heat solver parameters. Data taken from [Toolbox 2013].*

Assuming $\Delta x = \Delta y$, the equation (2) can be discretized using a *Forward in Time and Centered in Space scheme* into the following:

$$\frac{\partial u}{\partial t} = \frac{D}{c_s \rho c} \frac{u_{i+1,j} + u_{i-1,j} + u_{i,j+1} + u_{i,j-1} - 4u_{i,j}}{(\Delta x)^2} \quad (3)$$

which we can use along the structural springs directly (i.e. if there is a structural horizontal or vertical spring between two nodes, then there is a heat diffusion between those two nodes).

As the distance between nodes is quite small, the fraction dt/dx is too small to guarantee the stability of the system and convergence of this scheme. Using dimensional stability as a factor that influences the diffusion process we can keep the system stable. A higher dimensional stability c_s leads to a slower diffusion of the heat.

The nodes are updated with the new temperature slowly changing their state from not *burning* to *burning* then *burnout* due to heat and time. The *burning threshold* is set to 1.5 of the initial temperature (i.e. 768 ^oC). Then, a node burns and loses mass for a certain amount of time until only 20% of its original mass remains. Experimental Normalized Burn Rate (NBR) values for the combustion of briquettes can be found in [Chaney et al. 2010]. In our examples we used a burning rate of $0.02g.s^{-1}$. The node then becomes *burnout* and a candidate for fracture.

The burning of paper itself generates a flame and energy (s in equation (2)). When a node enters the *burning* state, a new fire emitter is created and attached to that node. The emitter is destroyed when the node enters the *burnout state*. Then it's temperature slowly decreases.

Lighting the Paper Before we start propagating the heat and the fire in the simulation, we need to add some energy to the system at the beginning of the simulation like a lighter would do on real paper. To add energy to the system, we attach a particle emitter to the lighter. The created particles then automatically add heat and external forces to the system.

4.3 Fibers Deformation

During the simulation the rest length of all *burning springs* is reduced by:

$$l(t + dt) = l(t) - \frac{factor * l_{init} * (T_a + T_b)}{k_s * c_s} \quad (4)$$

where l is the current rest length of the spring, l_{init} is its initial rest length, k_s is the spring stiffness, T_a and T_b are the temperature at the spring nodes and c_s is the dimensional stability. For a given temperature, a higher constant c_s and a higher stiffness k_s will make it more difficult to reduce the springs, which corresponds to a better paper quality. The temperature also takes part to the reduction of the springs: they are more easily reduced at higher temperatures. The *factor* constant is just a scaling factor that compensates for the low stiffnesses and c_s values. In our examples, *factor* varies between $1.e^{-12}$ and $50.e^{-12}$, depending on the paper type (the higher c_s, the higher *factor*).

A *burning spring* is a spring that has both particles in the burning state. As bending springs are longer, they also reduce by half when only one particle is in the burning state.

4.4 Paper Fracture

When an area of the paper is totally burnt, fractures can appear. A fracture appears when a non-elastic material is stretched too much. In our simulation, we break the bending springs that are totally burnt (i.e., both origin and target nodes are burnt) and elongated. In practice, we have found that using a threshold of 1.2% of the burnt rest length produced realistic results for all of the simulations. The burnt rest length is the value of the rest length of the spring when it enters the burnt state (i.e. the current value of l as computed with equation (4) when the spring changes from *burning* to *burnout* state).

When a burnt bending spring is stretched, it is removed from the simulation, and both the mass-spring system and the polygonal mesh used for rendering are opened in the perpendicular direction. All connections are updated (structural, diagonal and bending springs) and the polygonal mesh is modified (see figure 4 for a sketch).

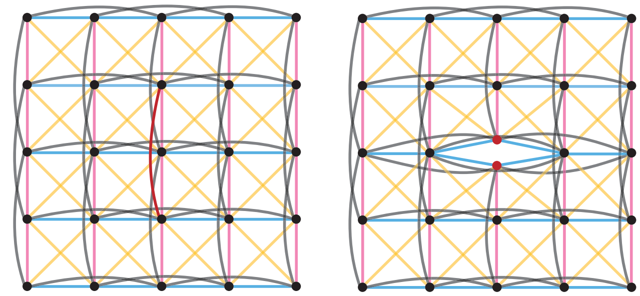

Figure 4: *Left: original mesh with structural springs (blue and pink), diagonal springs (yellow) and bending springs (black). In red, the burnt bending spring that is being cut. Right: resulting mesh after the fracture. The polygonal mesh uses the nodes as vertices and the structural springs as edges.*

Duplicating the Nodes and Connecting the Springs When a new cut is applied, the middle node of the bending spring is duplicated (nodes in red on figure 4 (right)). Some springs from the original node need to be unlinked and added to the new node:

1. Delete the bending spring that crosses the actual node. A vertical bending spring in the case of a horizontal cut and a horizontal bending spring in the case of a vertical cut.

2. Update the polygonal mesh.

3. Unlink the springs of one side from the old node and connect them to the new node and update diagonal springs.

4. Duplicate structural springs if necessary and add them to the new node.

5. Create new bending springs when necessary.

This algorithm for cutting the paper does not create new geometry and the new nodes do not take part to the diffusion process as they are already burnt, so it does not generate new computational cost to the simulation.

5 Results

Our examples were generated on an Intel Core 2 Duo 2.4GHz with 4GB of RAM processor and an NVIDIA GeForce 9400M graphics board under MacOSX 10.5 in interactive time. No optimization technique for the fire particles has been used to speed up the results.

Table 2 shows the parameters used for our simulations.

Size	Grammage	Density	Resolution	c_s
A4	$80g.m^{-2}$	$1500kg.m^{-3}$	32x48	$2e^{-4}$
A4	$400g.m^{-2}$	$1500kg.m^{-3}$	32x48	$100e^{-4}$

Table 2: *Parameters used in our simulations.*

Burning a Corner of a Sheet We first start a fire on a corner of a single sheet of standard $A4$ paper. One side of the sheet (here the cross direction) is attached so that the paper doesn't fall onto the floor or fly off. Figure 5 shows a frame of the beginning of the animation with and without flames and figure 6 shows the burning, crumpling and fracture of the paper as well as the corresponding mass-spring system.

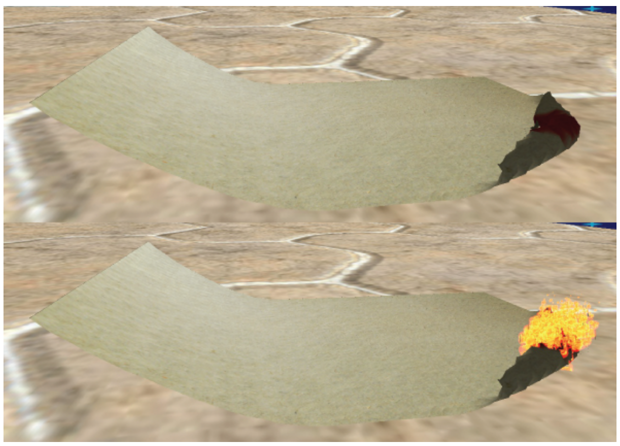

Figure 5: *Two frames of an animation: with and without flame rendering. The paper is a standard* $A4$ *$80g.m^{-2}$ sheet.*

Figure 6: *Two frames of the animation of a standard sheet of paper with fracture and a rendering of the corresponding mass-spring system. Left: paper is burning and starts to fracture; right: the burning process is over.*

Fake versus Real Figure 7 shows frames of two different animations and the comparison with real burnt paper.

Paper and Cardboard We compare the behavior of regular paper and cardboard. As paper has less weight it crumples more and fractures more than cardboard. Figure 8 shows a frame of a paper burning (top) and a cardboard burning (bottom) after the same amount of time. Note that the fire propagation is slower on the cardboard due to the higher dimentional stability and the fire front is also smaller on the cardboard because the grammage is higher and thus it is harder to consume.

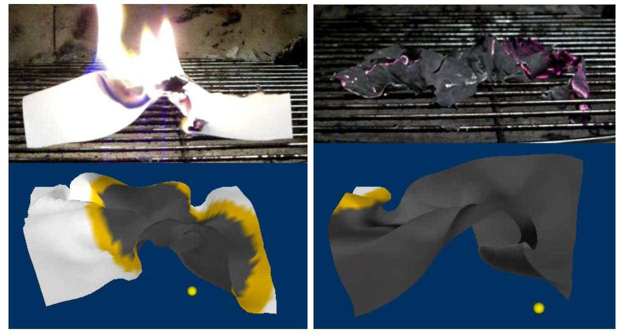

Figure 7: *Comparison between real paper burning and our simulation. Top: two pictures of real paper burning; bottom: two frames of the corresponding simulation using our mass-spring system combined to a heat diffusion solver generated at* 59 *fps without fracture and without fire particles.*

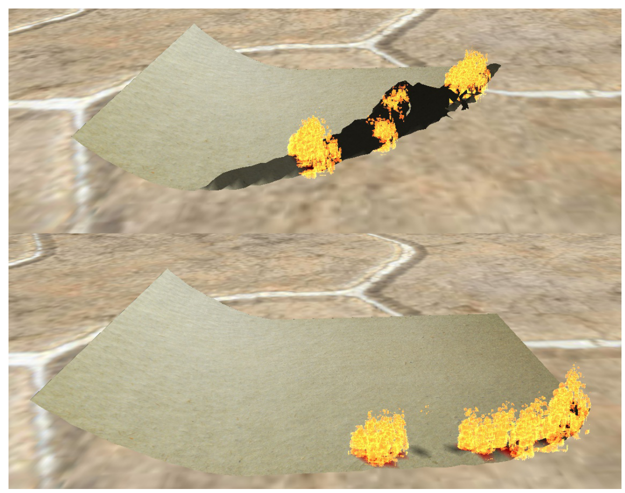

Figure 8: *Beginning of the simulation after burning the corner of the paper. Top: paper of* $80g.m^{-2}$ *and dimensional stability of* $2e^{-4}$*; bottom: cardboard of* $400g.m^{-2}$ *and dimensional stability of* $100e^{-4}$.

Stack of Sheets Because we simulate the fire with a particle system, we can burn a $3D$ stack of paper even though the internal heat propagation in the paper is a $2D$ solver (see teaser image).

Cigarette We simulated other paper shapes such as a cylinder. As the simulation is guided by the fibers and the heat diffusion is $2D$ along the fibers, it is not necessary to change anything to the simulation. Figures 9 and 10 show the simulation after lighting an empty cigarette paper and the result a few seconds later. The first example shows the burning of regular white cigarette paper while the second example shows the burning of rolling paper. Note that the only parameter that has changed between the two simulations is the dimensional stability. The bottom row of each figure shows a comparison with real footage.

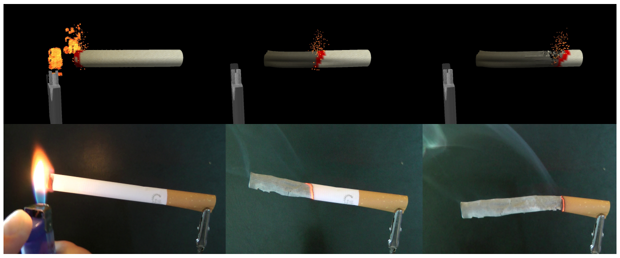

Figure 9: *Comparison of the burning of a real cigarette paper (top) with our simulation (bottom), with a grammage of $25g.m^{-2}$, a density of $700kg.m^{-3}$ and a stability $c_s = 80e^{-4}$. From left to right: beginning of the simulation after lighting an empty cigarette paper; the cigarette is a bit consumed a few seconds later; the cigarette starts to break at the same place in the simulation and in the video.*

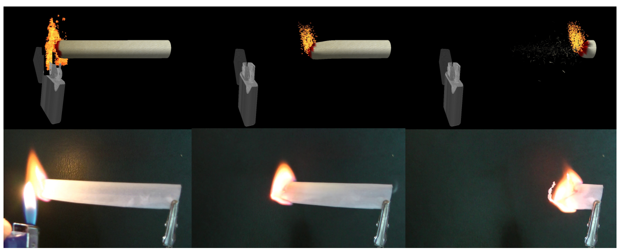

Figure 10: *Comparison of the burning of a real cigarette paper (top) with our simulation (bottom), with a grammage of $25g.m^{-2}$, a density of $700kg.m^{-3}$ and a stability $c_s = 5e^{-4}$. Both in the simulation and in reality, the paper turns entirely into ashes.*

6 Conclusion and Future Work

Our physically based technique simulates the crumpling, bending and burning of paper in interactive time. We used a mass-spring system where the springs distribution is similar to the fibers orientation, making it possible to map physical paper parameters to the simulation. In addition, the heat solver can be easily implemented on a regular grid using a discretized PDE. One of the limitations of the system is the tuning of the physical parameters, like in every physically based simulation. The paper parameters however can be easily chosen from real data.

At ideal conditions, i.e. without external forces and using a low initial temperature for burning (just start to burn and remove the lighter), the paper crumples and bends without breaking. However when it is burnt, the stress created by the adjacent burning area makes fractures appear naturally. Future work includes an improvement of the rendering of the quads from burnt paper to ashes.

As there is a direct mapping between springs connections and quads (primitive used for rendering) the cuts are currently only horizontal or vertical. Improving the cutting algorithm by adapting it to the burnt boundary is a goal for future work.

We simulate the fire using a particle system. The simulation is thus automatically fed with extra heat which keeps the paper burning after some time. To speed-up the computation, both the mass-spring system and the particle simulation could use an octree or a similar structure as the fire particle system is currently the bottleneck of the algorithm (10 fps with fire versus 60 fps without fire).

Our grid based solution is adapted to vertex and fragment shaders, thus implementing our algorithm on the GPU looks suitable in order to simulate finer and larger grids.

Finally, as the simulation is guided by fibers, it is possible to extend it to other materials made of fibers such as clothes or hair, opening new fields of investigation and use.

References

CARLSON, M., MUCHA, P., III, B. V. H., AND TURK, G. 2002. Melting and flowing. In *ACM SIGGRAPH Symposium on Computer Animation*.

CHANEY, J. O., CLIFFORD, M. J., AND WILSON, R. 2010. An experimental study of the combustion characteristics of low-density biomass briquettes. *Biomass magazine 1*.

JEONG, S., HYEONG KIM, T., AND KIM, C.-H. 2011. Shrinkage, wrinkling and ablation of burning cloth and paper. *The Visual Computer 27*, 6-8 (June), 417–427.

JOHANSSON, K., LUNDBERG, P., AND RYBERG, R. 2011. *Manual de produccion grafica. Recetas*.

LIU, S., LIU, Q., AN, T., SUN, J., AND PENG, Q. 2009. Physically based simulation of thin-shell objects' burning. *Vis. Comput. 25*, 5-7, 687–696.

LOSASSO, F., IRVING, G., GUENDELMAN, E., AND FEDKIW, R. 2006. Melting and burning solids into liquids and gases. *IEEE Transactions on Visualization and Computer Graphics 12*, 3, 343–352.

MATSUMURA, M., AND TSURUNO, R. 2006. Animating viscous fluids in the multiphase field. In *SIGGRAPH '06: ACM SIGGRAPH 2006 Research posters*, ACM, New York, NY, USA, 134.

MELEK, Z., AND KEYSER, J. 2003. Interactive simulation of burning objects. In *PG '03: Proceedings of the 11th Pacific Conference on Computer Graphics and Applications*, IEEE Computer Society, 462.

MELEK, Z., AND KEYSER, J. 2004. Modeling decomposing objects under combustion. In *VIS '04: Proceedings of the conference on Visualization '04*, IEEE Computer Society, 598.14.

MELEK, Z., AND KEYSER, J. 2006. Bending burning matches and crumpling burning paper. In *SIGGRAPH '06: ACM SIGGRAPH 2006 Research posters*, 131.

MELEK, Z., AND KEYSER, J. 2007. Driving object deformations from internal physical processes. In *SPM '07: Proceedings of the 2007 ACM symposium on Solid and physical modeling*, 51–59.

NEALEN, A., MÜLLER, M., KEISER, R., BOXERMAN, E., AND CARLSON, M. 2005. Physically based deformable models in computer graphics. In *Eurographics'05, State-of-the-Art Report*.

NGUYEN, D. Q., FEDKIW, R., AND JENSEN, H. W. 2002. Physically based modeling and animation of fire. *ACM Trans. Graph. 21*, 3 (July), 721–728.

PROVOT, X. 1995. Deformation constraints in a mass-spring model to describe rigid cloth behavior.

REEVES, W. T. 1983. Particle systems: a technique for modeling a class of fuzzy objects. *ACM Trans. Graph. 2*, 2 (Apr.), 91–108.

TOOLBOX, T. E., 2013. Resources, tools and basic information for engineering and design of technical applications !

VAN DER BURG, J., 2000. Building an advanced particle system, June.